

Bridging the Gap between the Sun and Sun-Like Stars: Universal Atmospheric Heating Mechanism and Empirical Reproduction of XUV Spectra

[Toriumi & Airapetian 2022, ApJ, 927, 179]



Shin Toriumi
ISAS/JAXA



Kosuke Namekata
NAOJ



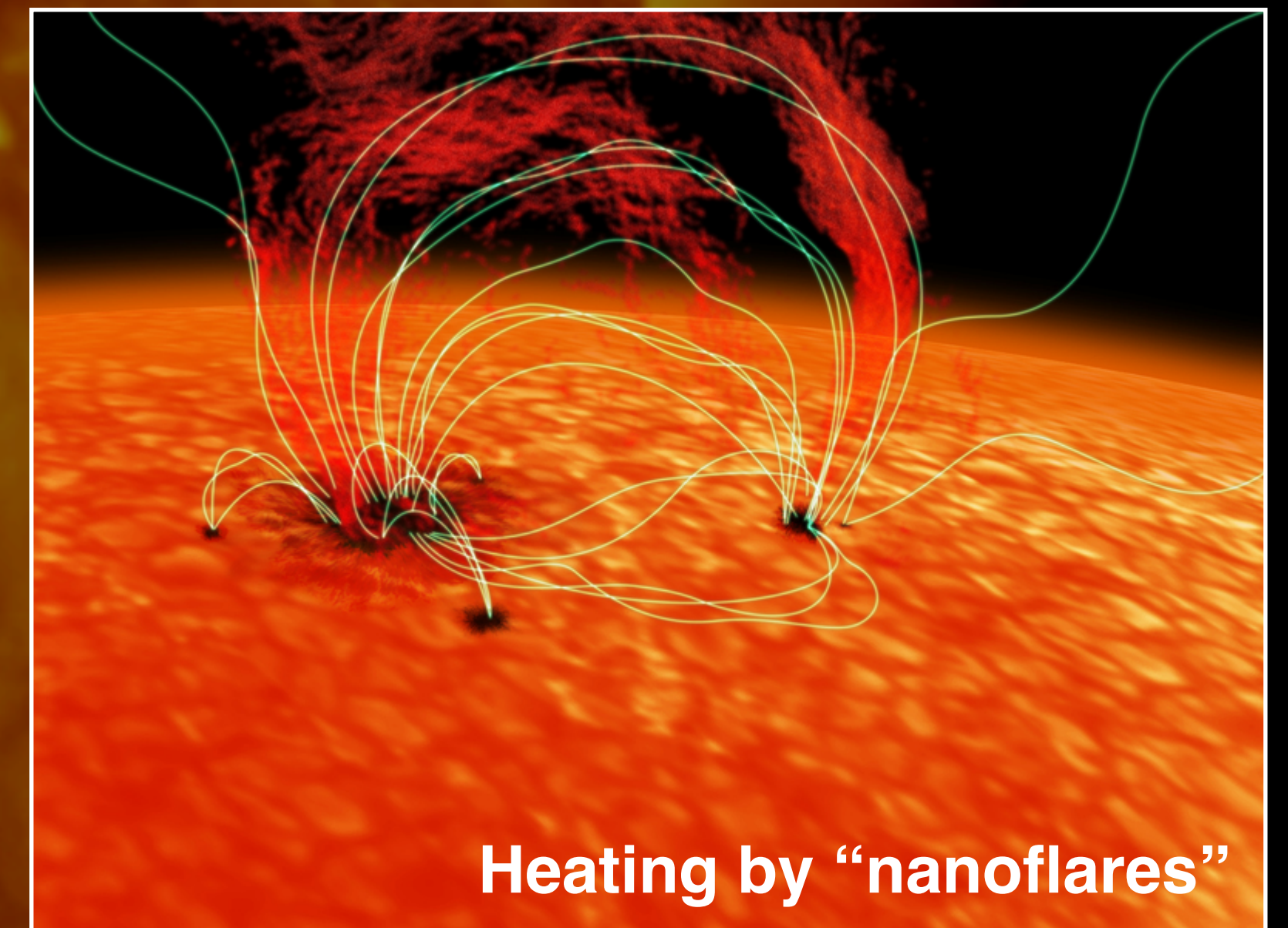
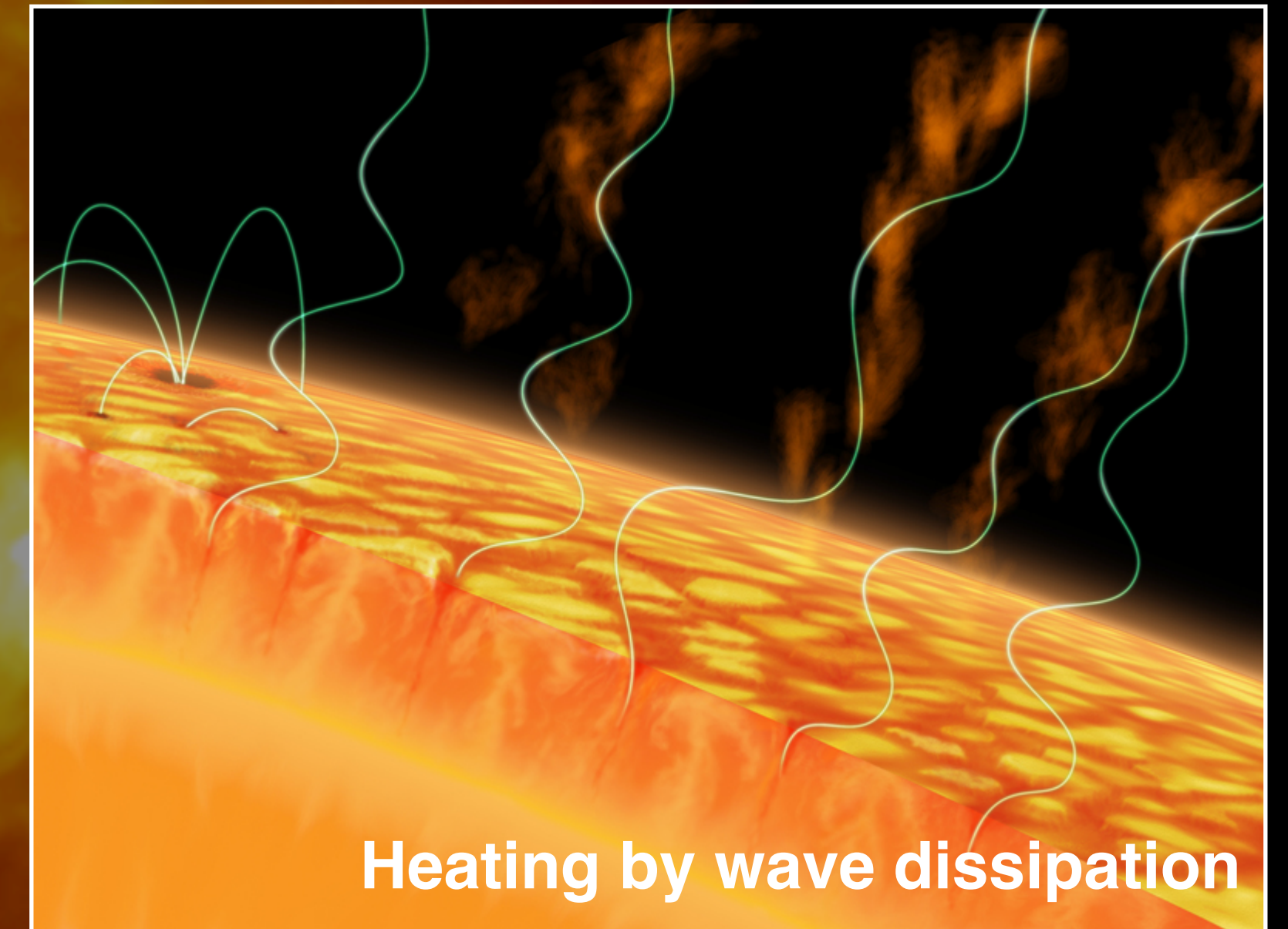
Vladimir Airapetian
NASA, American Univ



Yuta Notsu
CU Boulder, NSO, TITech

1. Introduction

- Extremely hot outer atmospheres
 - Corona > 1 MK / chromosphere $\sim 10,000$ K
 - Magnetic heating: magnetic flux transports energy from surface upwards¹
 - Exact mechanism still unclear²
 - Wave dissipation?³
 - Nanoflares?⁴



[1: Güdel 2004; 2: Withbroe & Noyes 1977, Klimchuk 2006]

[3: van Ballegooijen et al. 2011, Cranmer & van Ballegooijen 2005; 4: Parker 1972, 1988]

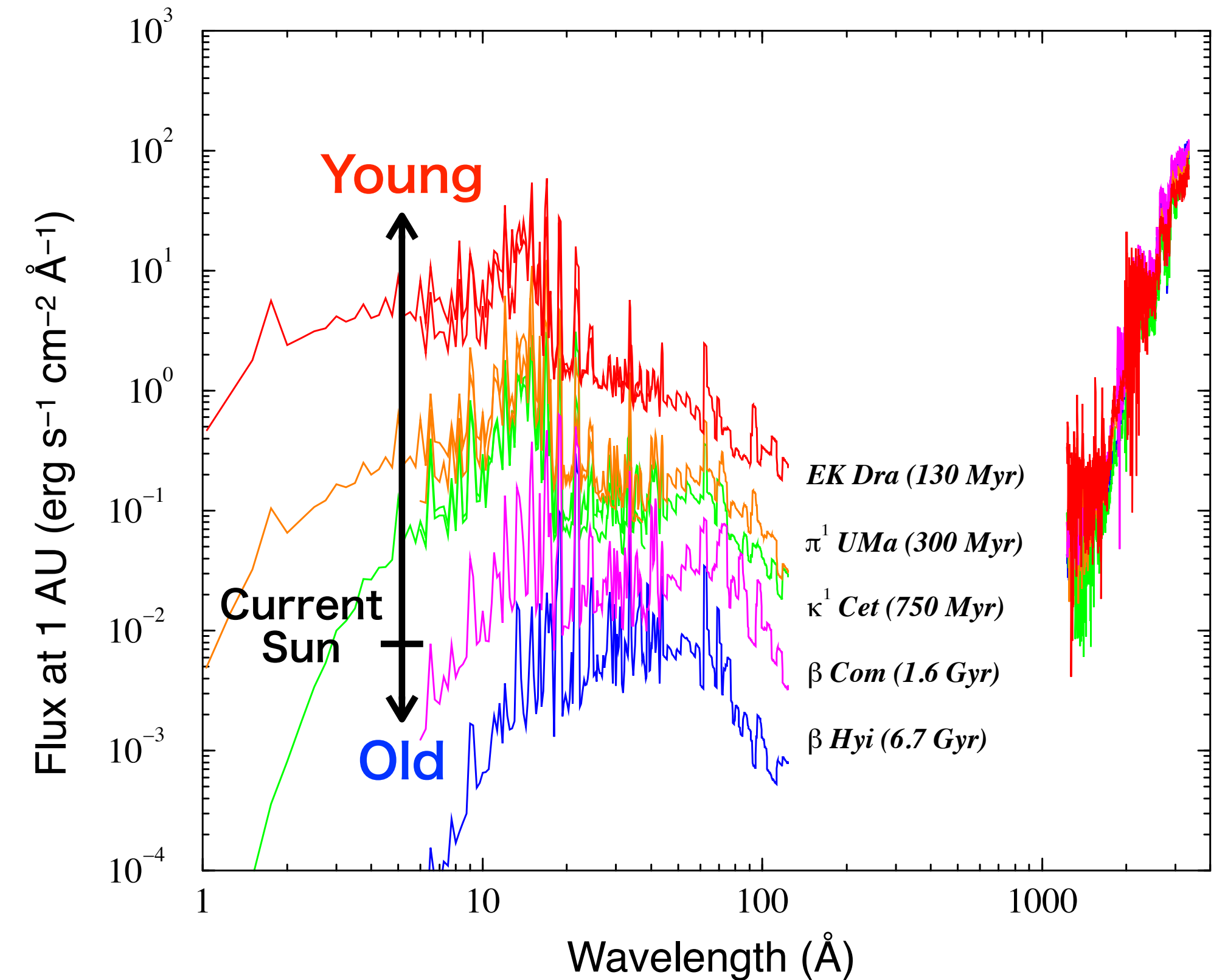
1. Introduction

- Extremely hot outer atmospheres

- Corona > 1 MK / chromosphere $\sim 10,000$ K
- Magnetic heating: magnetic flux transports energy from surface upwards¹
- Exact mechanism still unclear²
 - Wave dissipation?³
 - Nanoflares?⁴
- Young Sun and Sun-like stars
 - Strong XUV emission due to strong magnetic fields



Do the Sun and Sun-like stars share a common atmospheric heating mechanism?

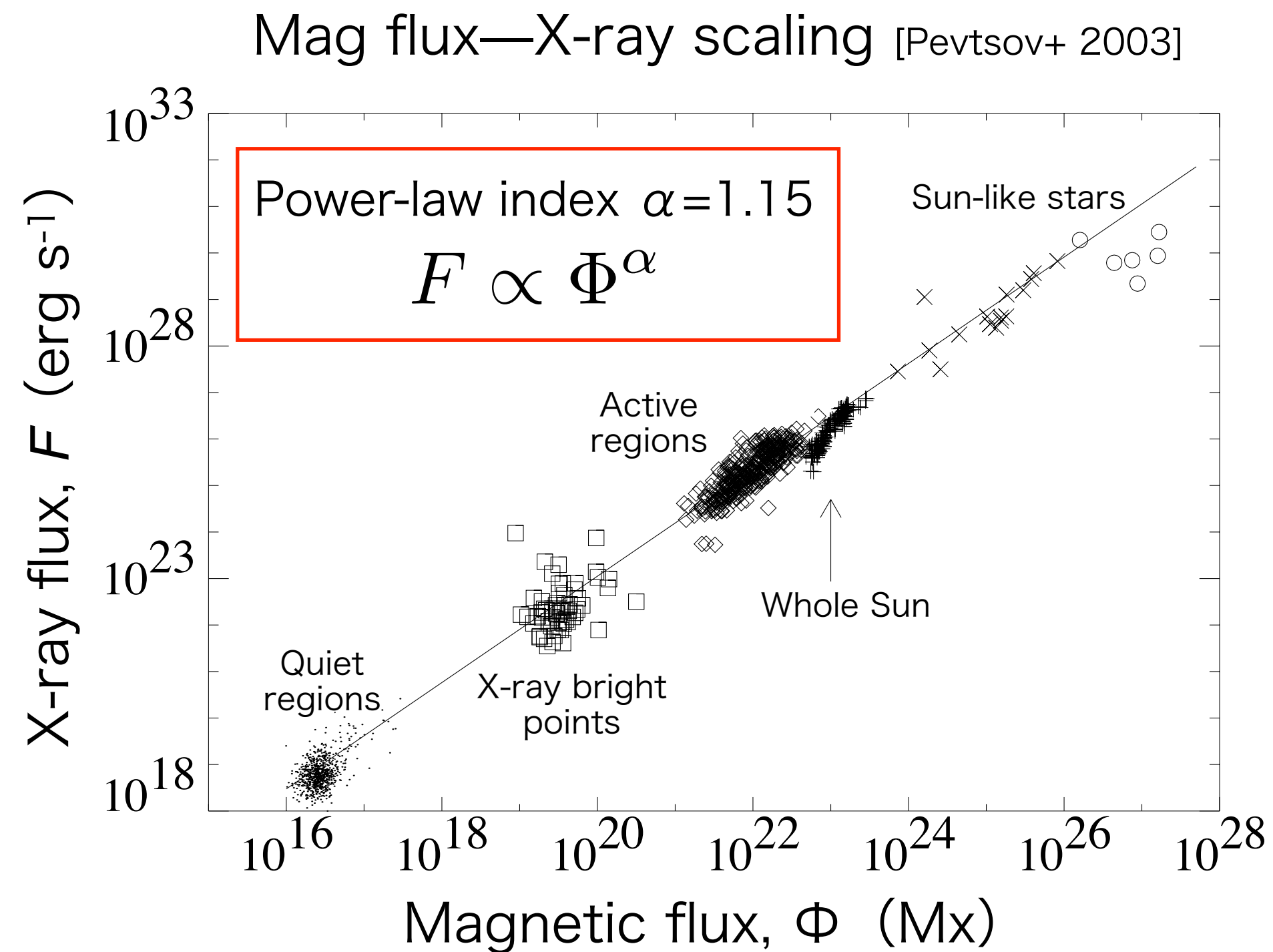


[Guinan & Ribas 2002]

[1: Güdel 2004; 2: Withbroe & Noyes 1977, Klimchuk 2006]

[3: van Ballegooijen et al. 2011, Cranmer & van Ballegooijen 2005; 4: Parker 1972, 1988]

1. Introduction



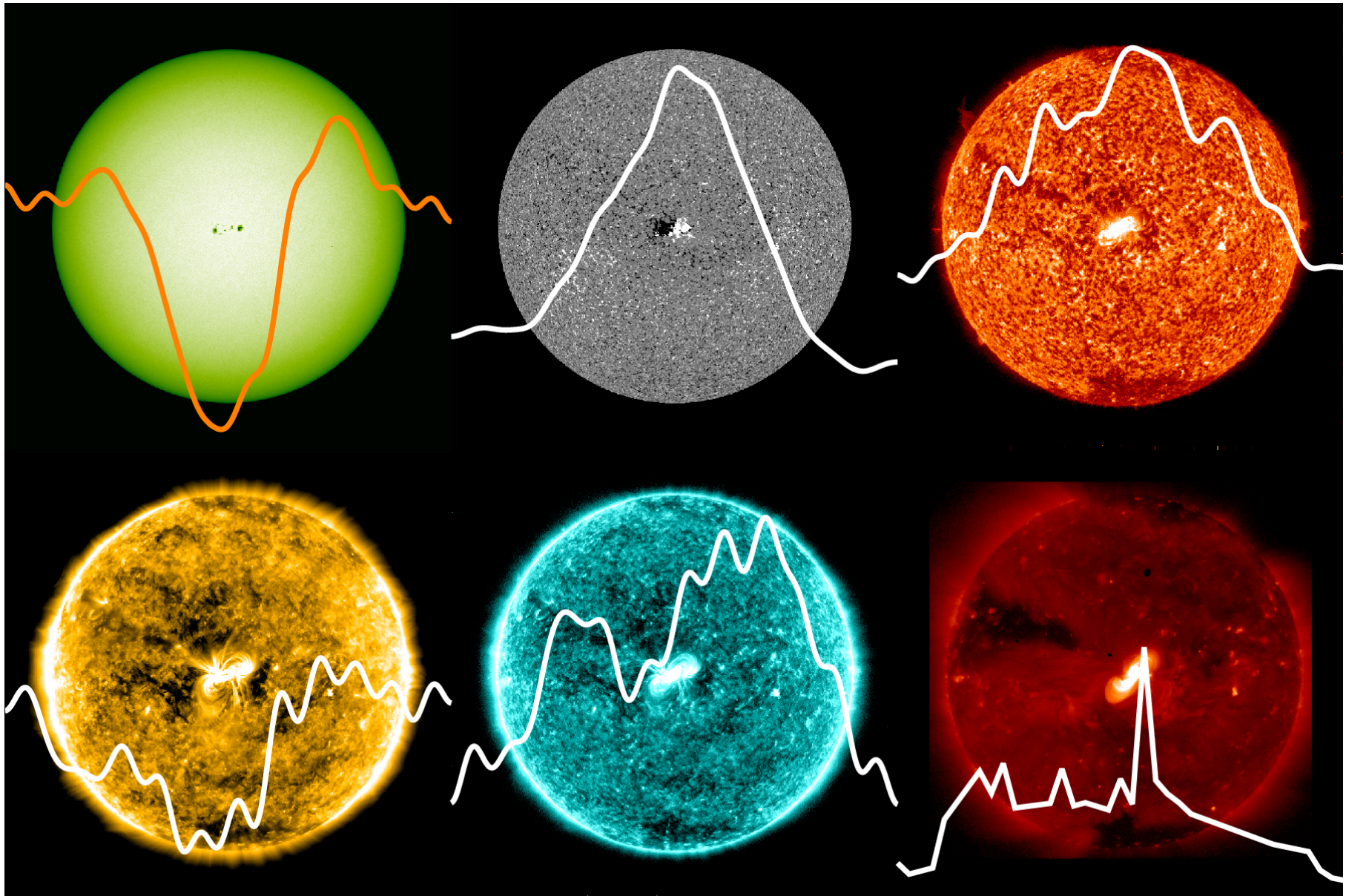
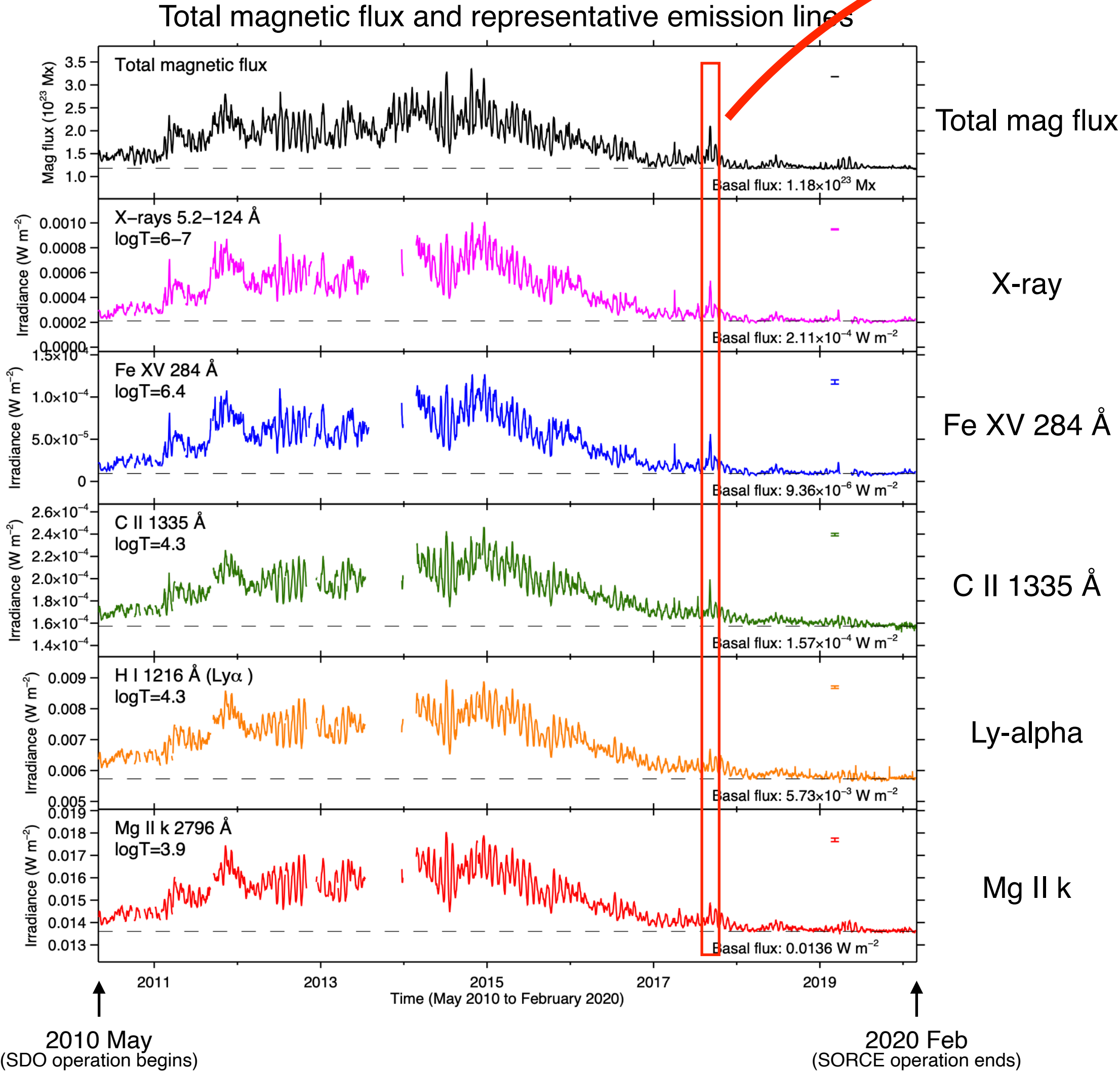
- Universality of atmospheric heating
 - X-ray luminosity has a uniform scaling relationship with a power-law index of $\alpha \approx 1.15$
 - One of the key Yohkoh results¹
 - Barometer for efficiency of coronal heating in regard to surface magnetic flux
- ▼
- What about in other lines (= temperatures)?²
 - Analysis of Sun-as-a-star synoptic data over 10 yr
 - X-ray, EUV, UV, optical, and radio
 - corresponding to corona ($\log T=6-7$) to chromosphere ($\log T=4$)
 - Compare scaling with stellar data

[1: Fisher+ 1998; Pevtsov+ 2003; Vidotto+ 2014]

[2: Skumanich 1975; Schrijver+ 1989; Rutten+ 1991; Loukitcheva+ 2009; Barczynski+ 2018]

2. Analysis

- Solar synoptic data over 10 yr



Each spike corresponds to sunspot transit
[e.g. Toriumi et al. 2020]

Total radial unsigned magnetic flux

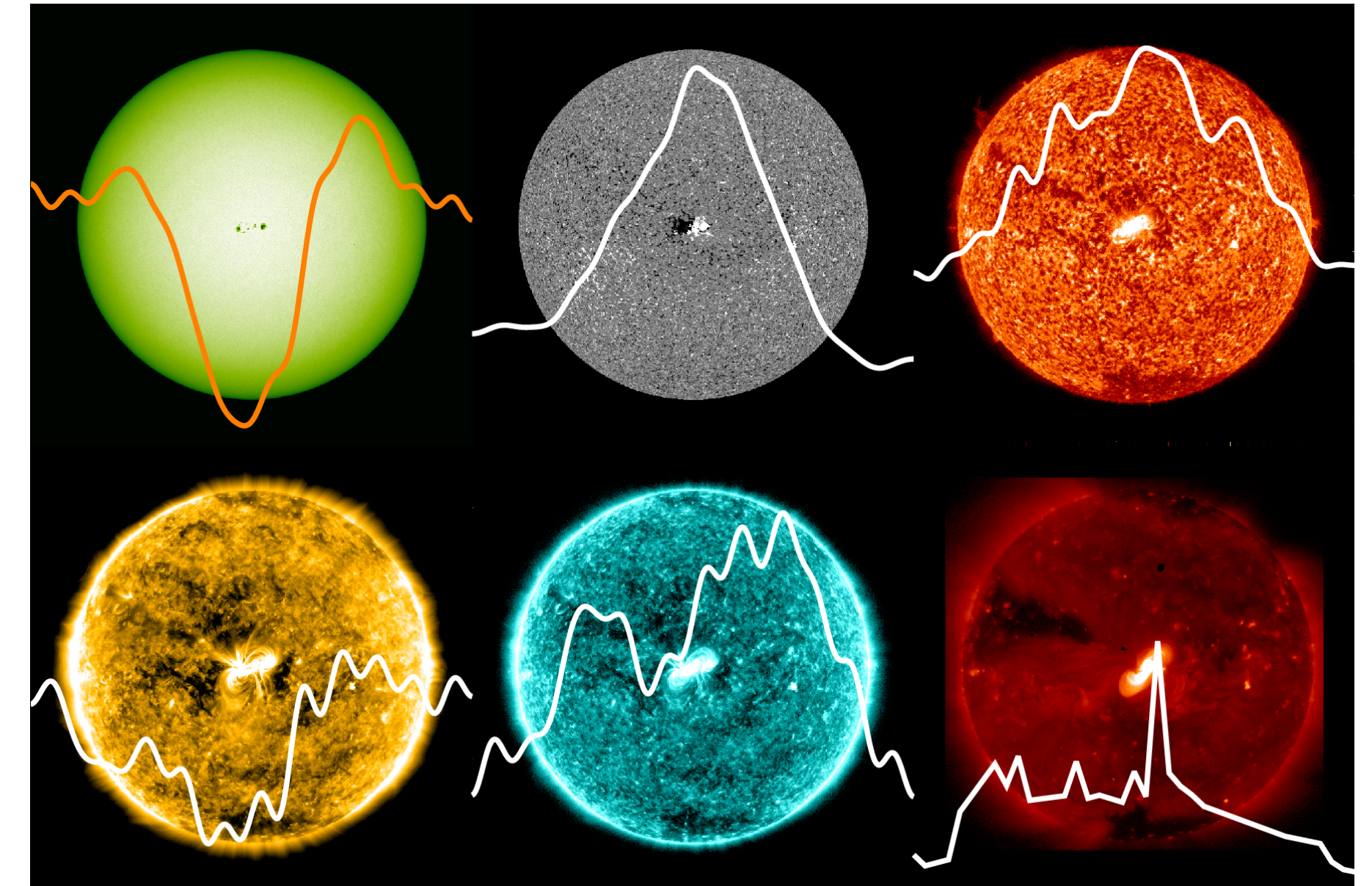
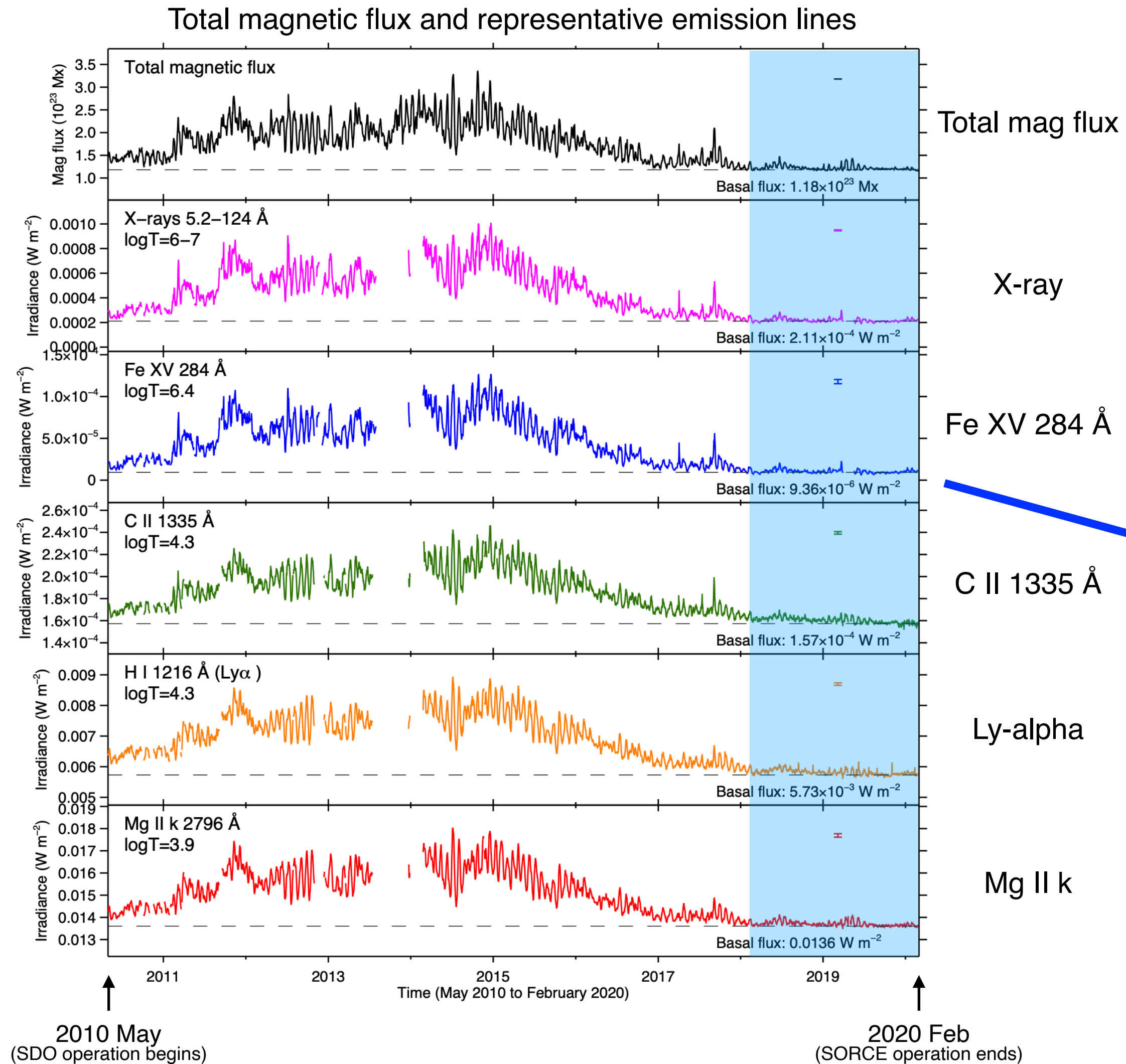
- daily value
- generated from four full-disk line-of-sight magnetograms per day

16 spectral lines/bands

- daily value
- X-ray to radio
- $\log T=3.8-7$

2. Analysis

- Solar synoptic data over 10 yr



Each spike corresponds to sunspot transit
[e.g. Toriumi et al. 2020]

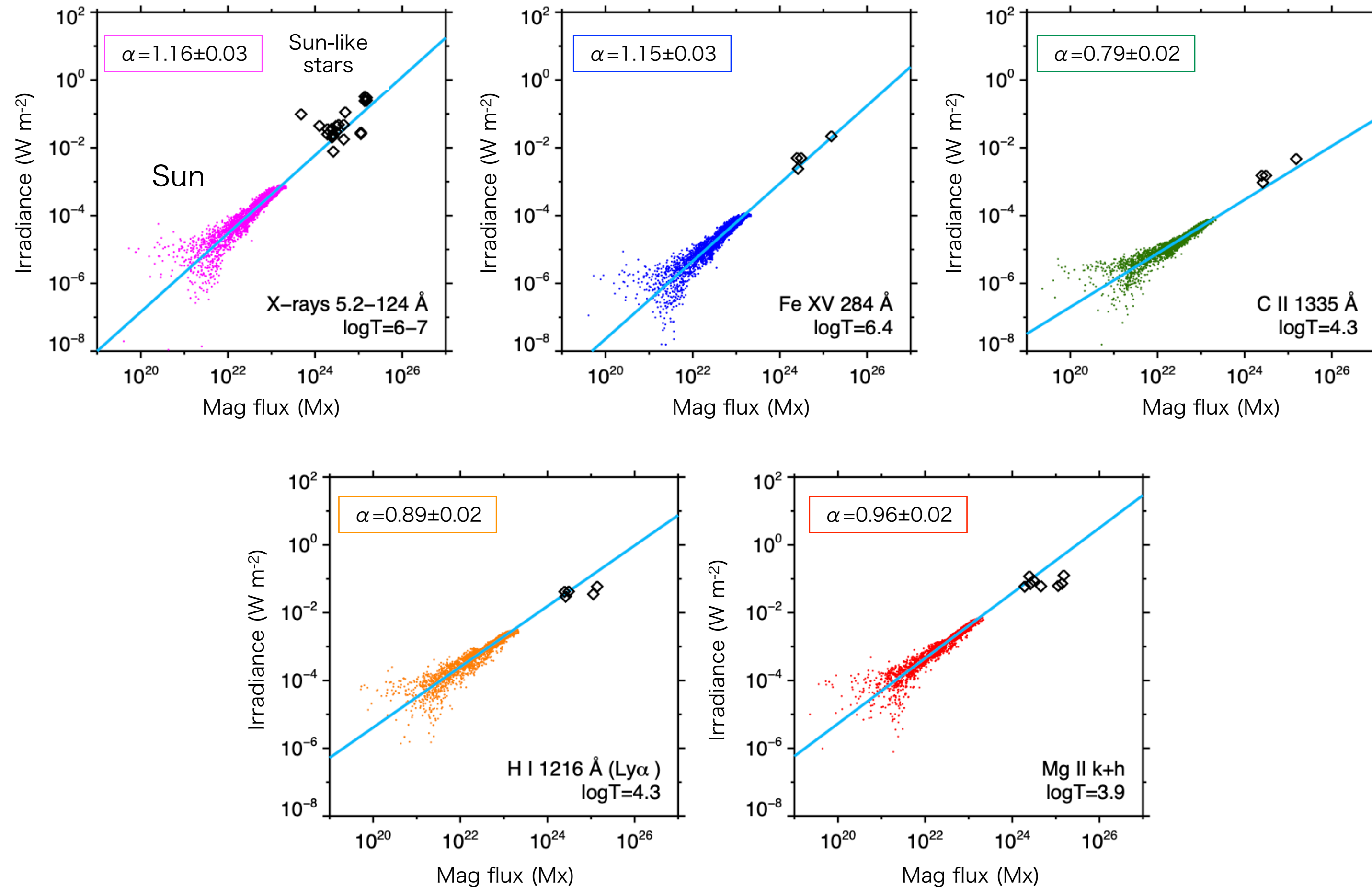
- Calculate basal flux and residual
 - Basal fluxes are defined as medians of data from Mar 2019 to Feb 2020 with following criteria
 - Sunspot number = 0
 - Total sunspot area = 0
 - Magnetic flux < 5th percentile of all time

$$\text{Residual} = \text{Light curve} - \text{Basal flux}$$

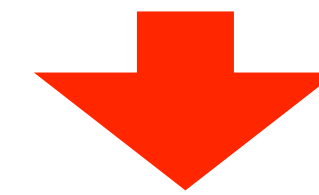
- Basal flux: background heating
- Residual: heating due to magnetic elements

3. Results

Mag flux—multi-line proportionality $F \propto \Phi^\alpha$



- **Stellar data**
 - Mainly G-dwarfs with ages from 50 Myr to 4.5 Gyr
 - Total magnetic flux based on Kochukhov et al. (2020)
 - Irradiance from published data
- **X-rays**
 - $\alpha=1.16$ is consistent with Yokoh results
 - Stellar data are located on the extensions of the solar power-law relation
- **Other lines**
 - Power-law scalings are consistent between the Sun and Stars at any wavelengths (= temperatures)



✓ Heating mechanism is universal among the Sun and stars, regardless of age or activity



Sun

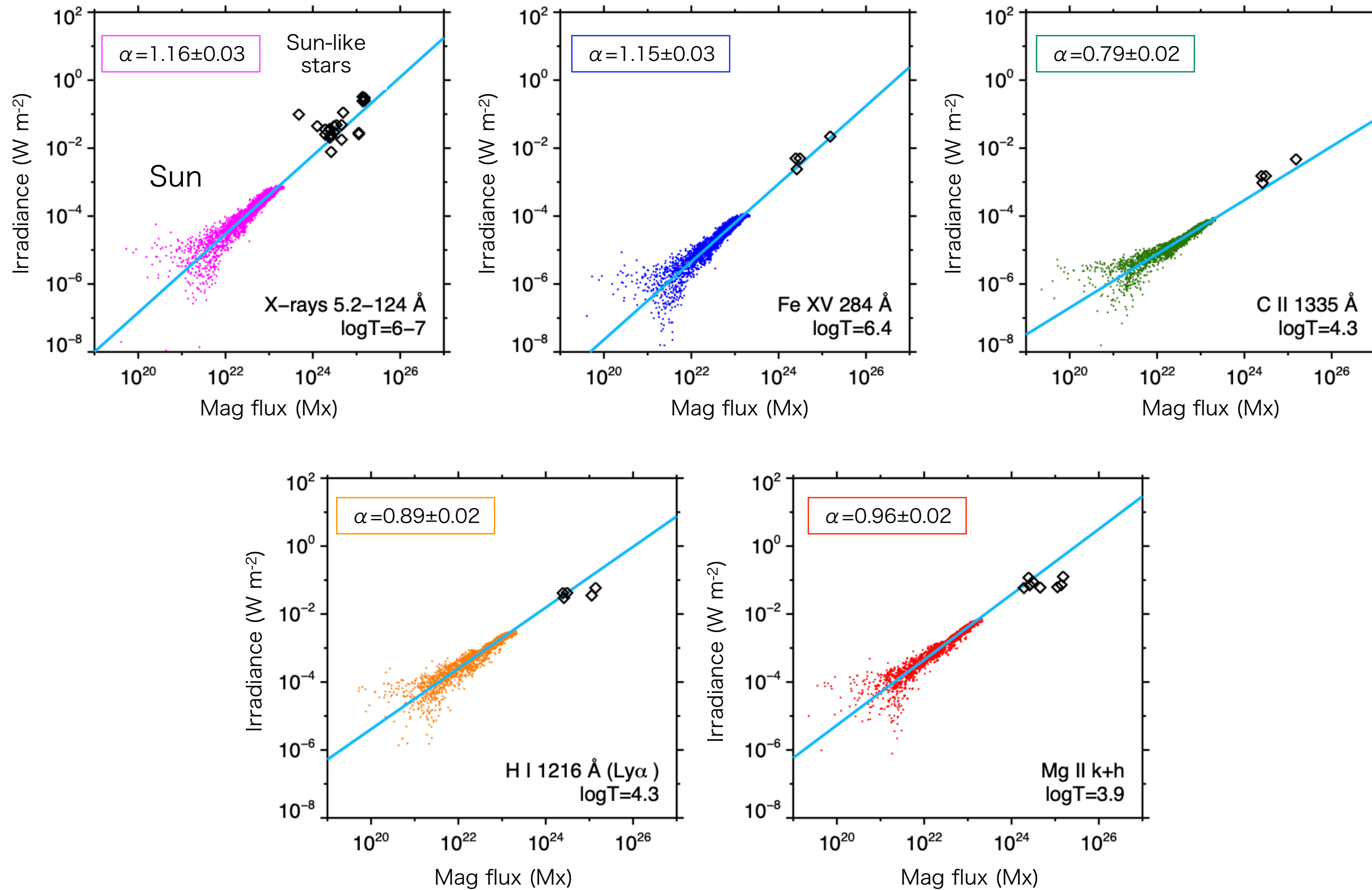
the
ivity

8

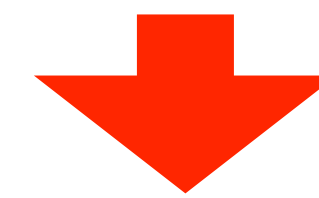
References. Turon et al. (1993), Valenti & Fischer (2005), McDonald et al. (2012), Gonzalez et al. (2010), Cole et al. (2015), Allende Prieto & Lambert (1999), Vidotto et al. (2014), Rosén et al. (2016), Oláh et al. (2016), See et al. (2019), Kochukhov et al. (2020), Telleschi et al. (2005), Ribas et al. (2005), Takeda et al. (2007), Wood & Linsky (2010), Güdel et al. (1997), Wood et al. (2005), Schmitt et al. (1990), Dorren & Guinan (1994).

3. Results

Mag flux—multi-line proportionality $F \propto \Phi^\alpha$

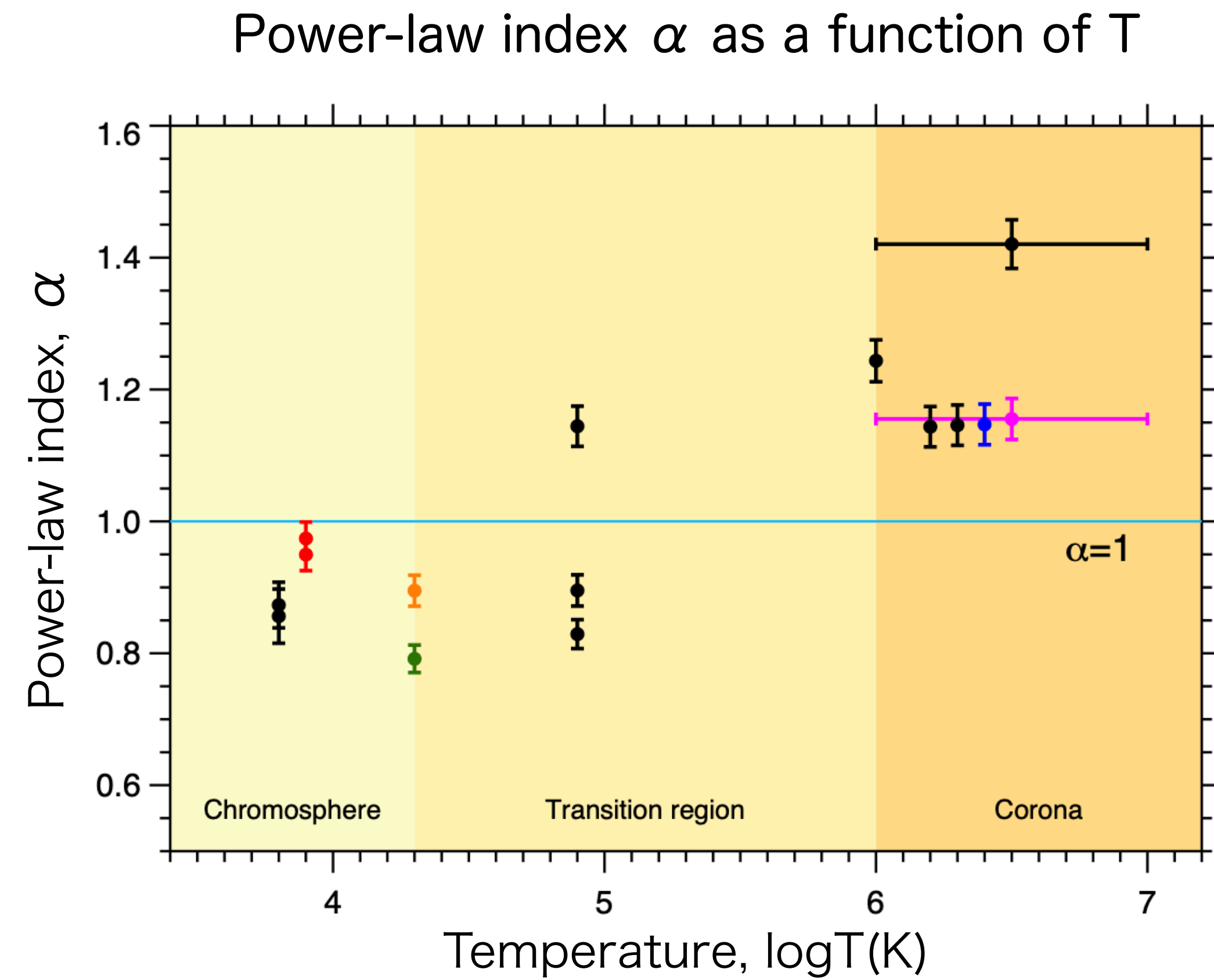


- **Stellar data**
 - Mainly G-dwarfs with ages from 50 Myr to 4.5 Gyr
 - Total magnetic flux based on Kochukhov et al. (2020)
 - Irradiance from published data
- **X-rays**
 - $\alpha=1.16$ is consistent with Yokoh results
 - Stellar data are located on the extensions of the solar power-law relation
- **Other lines**
 - Power-law scalings are consistent between the Sun and Stars at any wavelengths (= temperatures)

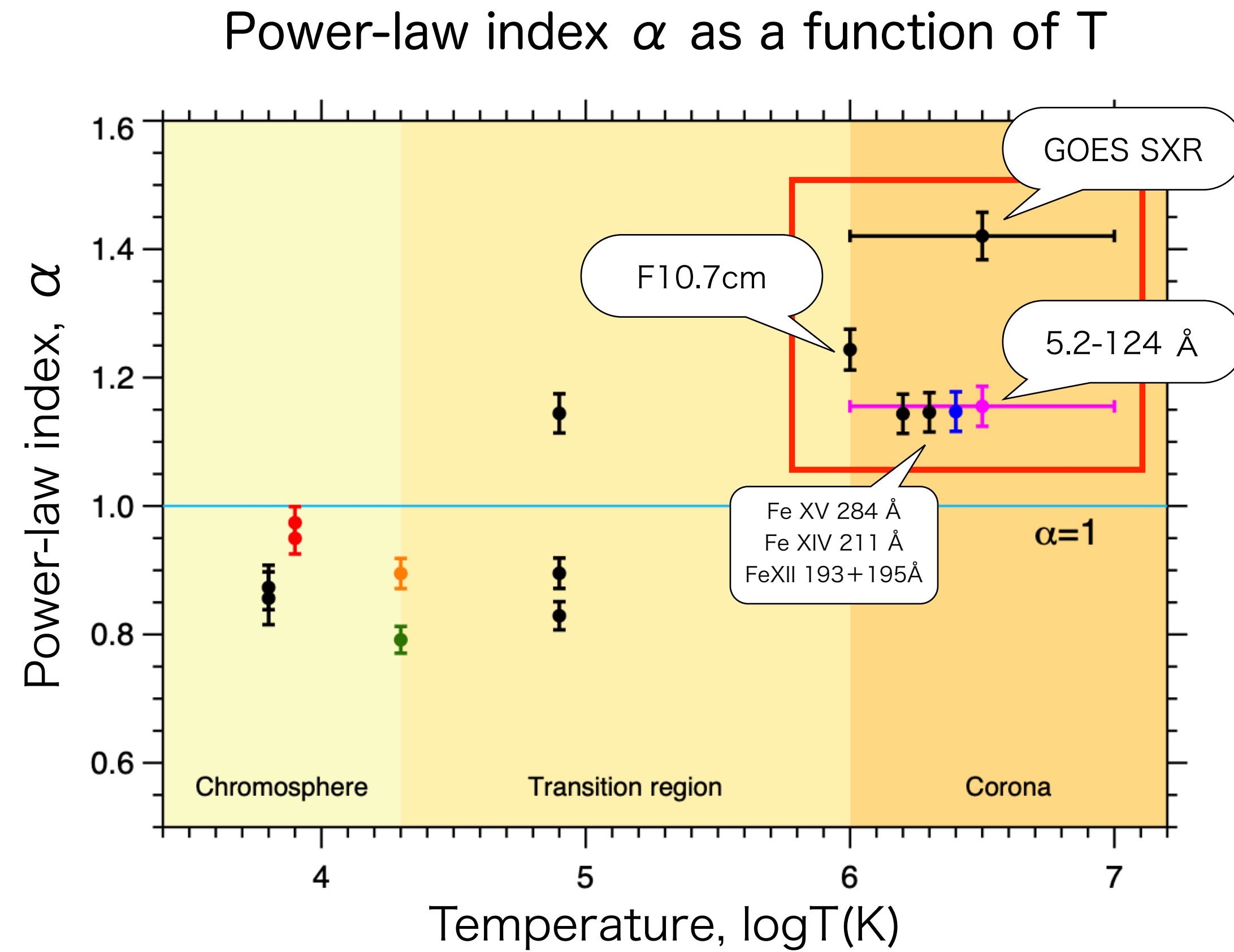


✓ Heating mechanism is universal among the Sun and stars, regardless of age or activity

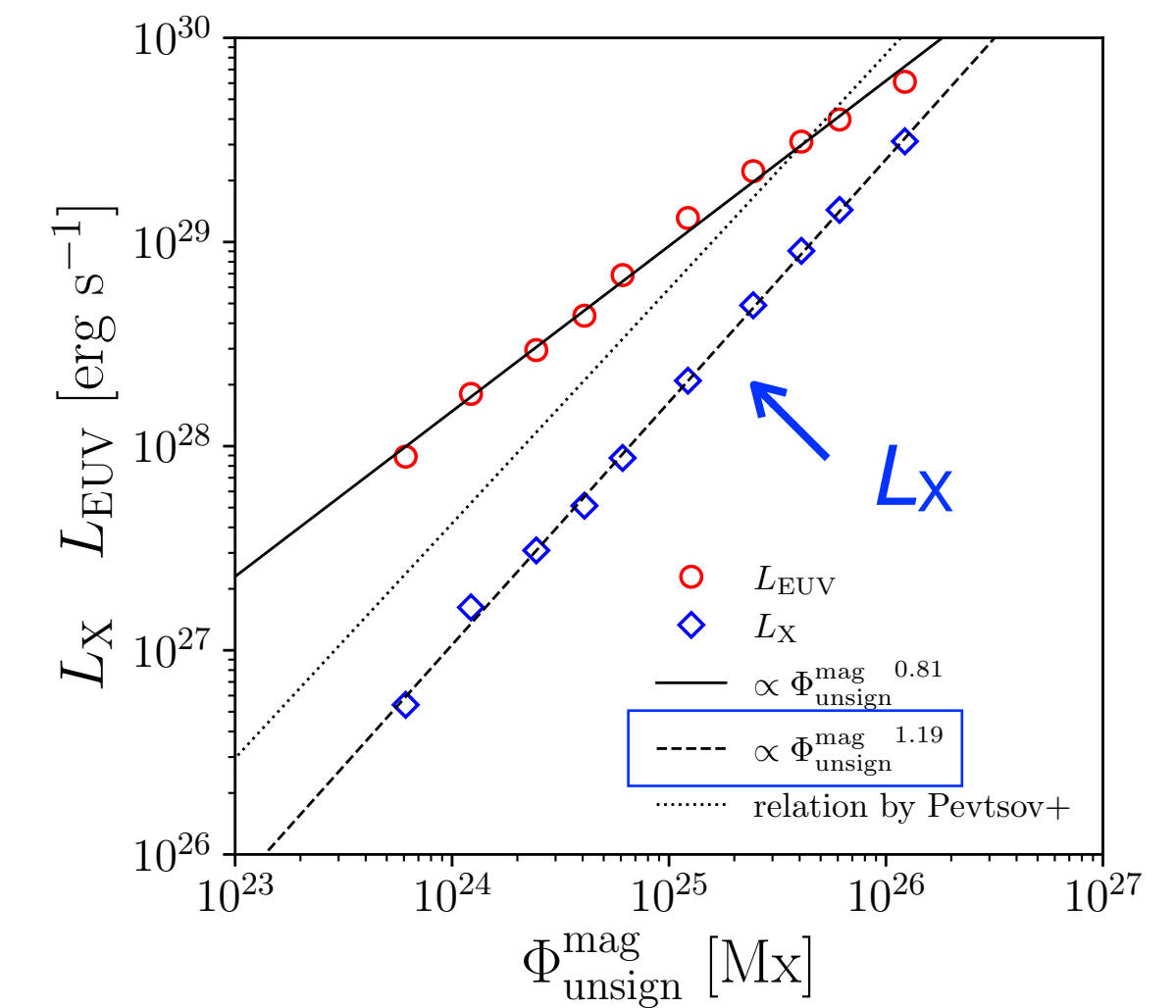
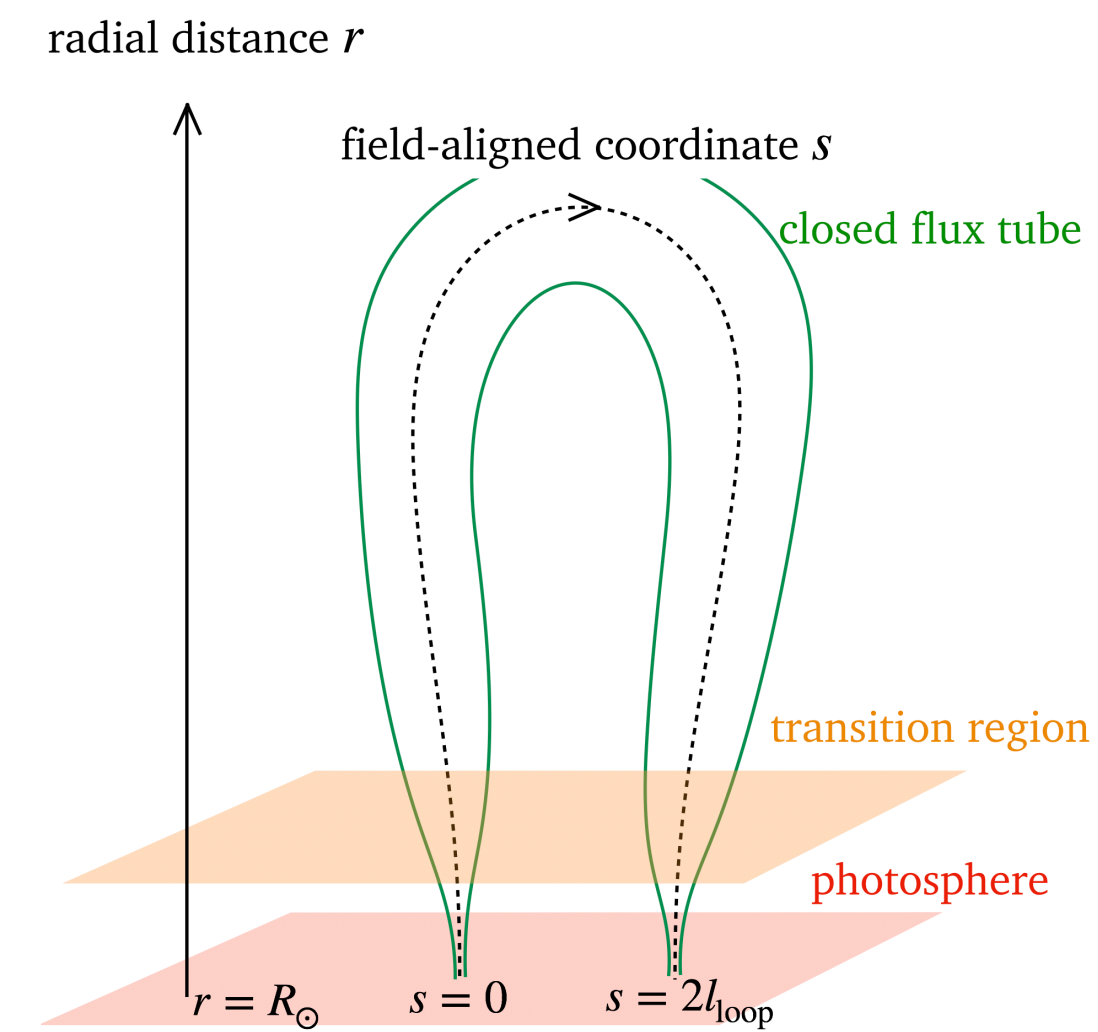
3. Results



3. Results



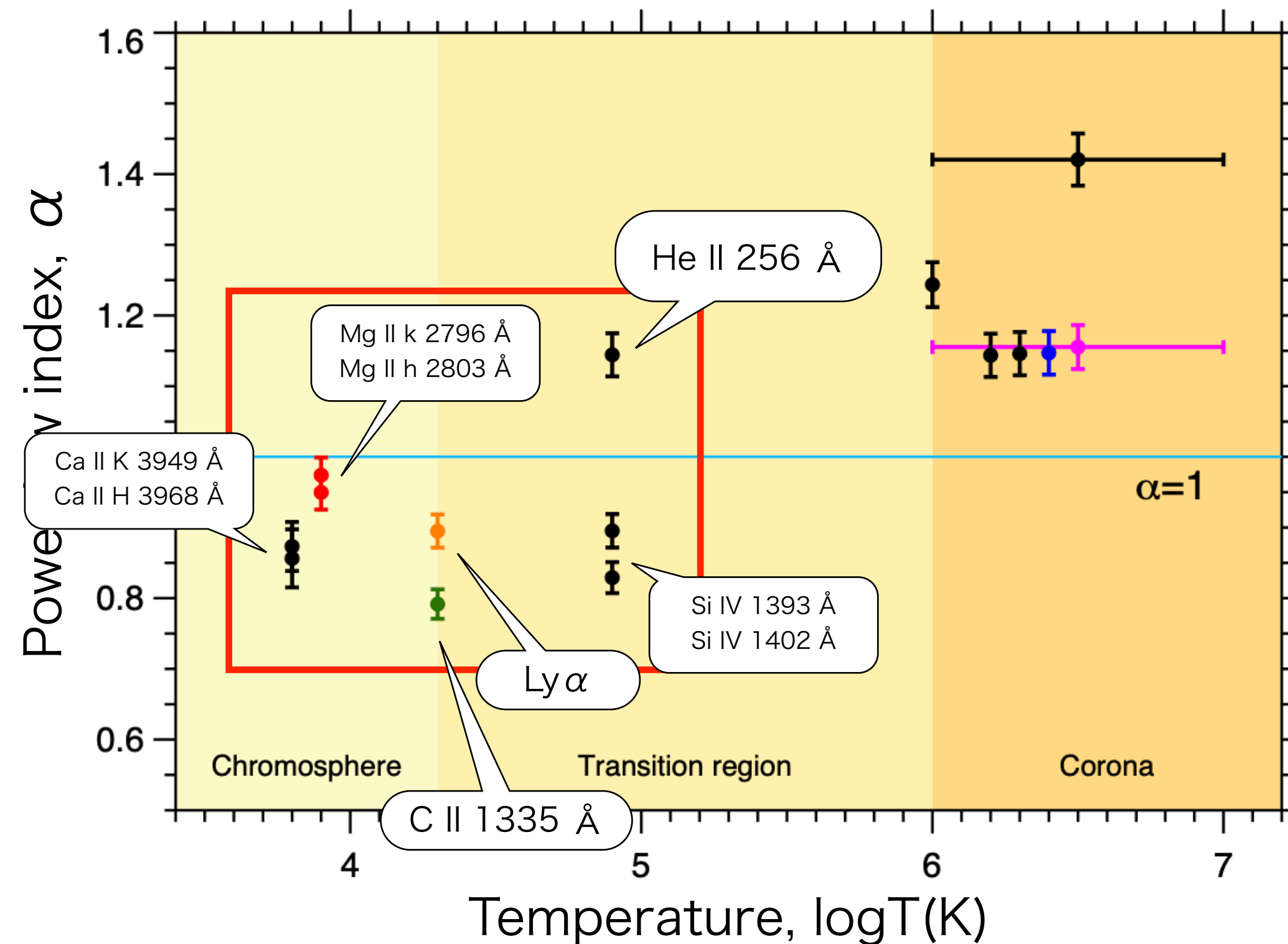
- Corona: $\log T > 6$
 - Not only X-rays but also **other coronal proxies consistently show $\alpha > 1$**
 - Explained by theoretical and numerical models [Zhuleku et al. 2020; also Fisher+1998; Takasao+ 2020]



[Shoda & Takasao 2020]

3. Results

Power-law index α as a function of T



- Corona: $\log T > 6$
 - Not only X-rays but also **other coronal proxies consistently show $\alpha > 1$**
 - Explained by theoretical and numerical models [Zhuleku et al. 2020; also Fisher+1998; Takasao+ 2020]
- TR to chromosphere: $\log T < 6$
 - **Power-law exponents fall below unity, $\alpha < 1$** , indicating that the efficiency of atmospheric heating is weaker than the corona
 - Explanation using a simple geometrical model [Schrijver et al. 1989]
 - For numerical modeling, chromospheric radiative transfer may be needed

3. Results

Power-law index α as a function of T

- Line number is greatly increased
 - Allows for close inspection of temperature dependence

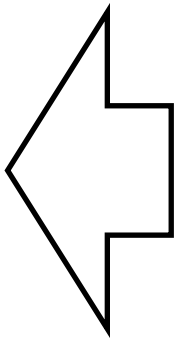
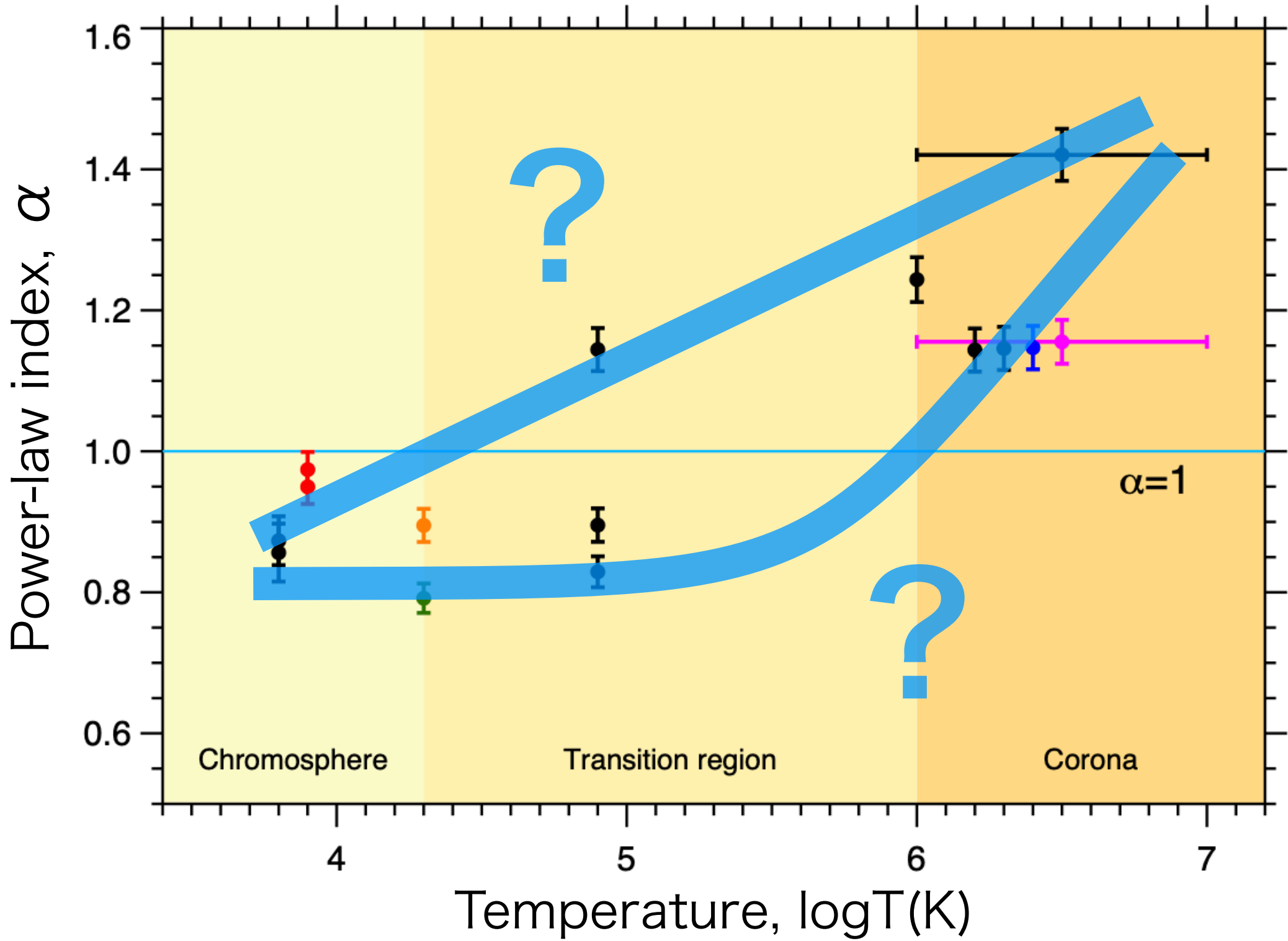


Table 1. Summary of the observables

Feature	log (T/K)	Wavelength (Å)	Basal	Minimum	Maximum	Unit	Source
(1)	(2)	(3)	(4)	(5)	(6)	(7)	(8)
Radial magnetic flux	3.8	6173.3	1.18×10^{23}	1.16×10^{23}	3.35×10^{23}	Mx	SDO/HMI
LOS magnetic flux	3.8	6173.3	7.02×10^{22}	6.85×10^{22}	2.52×10^{23}	Mx	SDO/HMI
Sunspot number	3.8	WL	0	0	220	–	WDC-SILSO (ver 2.0)
Sunspot area	3.8	WL	0	0	3120	MSH	USAF/NOAA
F10.7cm radio	~6	10.7×10^8	68.83	63.67	466.57	sfu	DRAO
X-rays 1–8 Å	6–7	1–8	0	1.00×10^{-9}	4.81×10^{-5}	W m ⁻²	GOES/XRS
X-rays 5.2–124 Å	6–7	5.2–124	2.11×10^{-4}	1.85×10^{-4}	1.01×10^{-3}	W m ⁻²	SORCE/XPS
X-rays (XRT)	6.8	–	5.00×10^{-5}	4.63×10^{-5}	1.01×10^{-3}	W m ⁻²	Hinode/XRT
Fe XV 284 Å	6.4	284.15 ± 1.50	9.36×10^{-6}	5.68×10^{-6}	1.27×10^{-4}	W m ⁻²	SORCE/XPS
Fe XIV 211 Å	6.3	211.32 ± 1.50	1.20×10^{-5}	9.88×10^{-6}	6.75×10^{-5}	W m ⁻²	SORCE/XPS
Fe XII 193+195 Å	6.2	193.50 ± 2.50	6.16×10^{-5}	5.66×10^{-5}	1.72×10^{-4}	W m ⁻²	SORCE/XPS
Fe XII 1349 Å	6.2	1349.40 ± 1.00	3.64×10^{-6}	3.23×10^{-6}	5.66×10^{-6}	W m ⁻²	SORCE/SOLSTICE
Fe X 174 Å	6.1	174.53 ± 1.50	5.64×10^{-5}	5.40×10^{-5}	0.90×10^{-4}	W m ⁻²	SORCE/XPS
Fe XI 180 Å	6.1	180.41 ± 1.50	4.57×10^{-5}	4.31×10^{-5}	0.95×10^{-4}	W m ⁻²	SORCE/XPS
F10.7cm radio	~6	10.7×10^8	68.83	63.67	466.57	sfu	DRAO
Fe IX 171 Å	5.9	171.07 ± 1.50	5.50×10^{-5}	5.32×10^{-5}	0.73×10^{-4}	W m ⁻²	SORCE/XPS
N V 1238 Å	5.3	1238.90 ± 1.15	1.62×10^{-5}	1.55×10^{-5}	2.39×10^{-5}	W m ⁻²	SORCE/SOLSTICE
N V 1242 Å	5.3	1242.95 ± 1.00	1.04×10^{-5}	9.89×10^{-6}	1.54×10^{-5}	W m ⁻²	SORCE/SOLSTICE
C IV 1548 Å	5.1	1548.25 ± 1.20	1.11×10^{-4}	1.07×10^{-4}	1.53×10^{-4}	W m ⁻²	SORCE/SOLSTICE
C IV 1551 Å	5.1	1550.73 ± 0.95	6.58×10^{-5}	6.38×10^{-5}	9.02×10^{-5}	W m ⁻²	SORCE/SOLSTICE
C III 1175 Å	5.0	1175.70 ± 1.75	5.52×10^{-5}	5.35×10^{-5}	8.24×10^{-5}	W m ⁻²	SORCE/SOLSTICE
He II 256 Å+blends	4.9	256.30 ± 3.00	5.53×10^{-5}	5.20×10^{-5}	1.21×10^{-4}	W m ⁻²	SORCE/XPS
He II 304 Å	4.9	304.00 ± 1.00	4.25×10^{-4}	4.09×10^{-4}	6.19×10^{-4}	W m ⁻²	SORCE/XPS
Si IV 1393 Å	4.9	1393.85 ± 1.30	4.45×10^{-5}	4.27×10^{-5}	7.66×10^{-5}	W m ⁻²	SORCE/SOLSTICE
Si IV 1402 Å	4.9	1402.85 ± 0.85	2.32×10^{-5}	2.25×10^{-5}	3.91×10^{-5}	W m ⁻²	SORCE/SOLSTICE
Si III 1206 Å	4.8	1206.60 ± 1.25	8.59×10^{-5}	8.32×10^{-5}	1.66×10^{-4}	W m ⁻²	SORCE/SOLSTICE
He I 10830 Å	4.5	10830.40 ± 0.25	0.0292	0.0270	0.0308	W m ⁻²	SORCE/SIM & SOLIS/ISS
C II 1335 Å	4.3	1335.25 ± 1.90	1.57×10^{-4}	1.52×10^{-4}	2.46×10^{-4}	W m ⁻²	SORCE/SOLSTICE
H I 1216 Å (Lyα)	4.3	1215.70 ± 2.00	5.73×10^{-3}	5.60×10^{-3}	8.94×10^{-3}	W m ⁻²	SORCE/SOLSTICE
O I 1302 Å	4.2	1302.20 ± 0.85	4.16×10^{-5}	3.93×10^{-5}	5.40×10^{-5}	W m ⁻²	SORCE/SOLSTICE
O I 1305 Å	4.2	1305.50 ± 1.75	9.14×10^{-5}	8.77×10^{-5}	1.17×10^{-4}	W m ⁻²	SORCE/SOLSTICE
Mg II k 2796 Å	(3.9)	2796.38 ± 0.78	0.0136	0.0135	0.0180	W m ⁻²	SORCE/SOLSTICE
Mg II h 2803 Å	(3.9)	2803.48 ± 0.65	0.0097	0.0096	0.0126	W m ⁻²	SORCE/SOLSTICE
Cl I 1351 Å	(3.8)	1305.50 ± 1.75	9.06×10^{-6}	8.57×10^{-6}	1.17×10^{-5}	W m ⁻²	SORCE/SOLSTICE
Ca II K 3934 Å	(3.8)	3933.66 ± 0.50	0.0114	0.0111	0.0130	W m ⁻²	SORCE/SIM & SOLIS/ISS
Ca II H 3968 Å	(3.8)	3968.47 ± 0.50	0.0139	0.0139	0.0155	W m ⁻²	SORCE/SIM & SOLIS/ISS
H I 6563 Å (Hα)	(3.8)	6562.80 ± 0.50	0.0369	0.0360	0.0448	W m ⁻²	SORCE/SIM & SOLIS/ISS
Ca II 8542 Å	(3.8)	8542.10 ± 0.50	0.0347	0.0346	0.0392	W m ⁻²	SORCE/SIM & SOLIS/ISS

NOTE—The first column shows the features, i.e., the total unsigned radial magnetic flux and the spectral lines. The second and third columns provide the formation temperature and wavelength range, respectively, for the measurement of irradiance. The temperatures are obtained from the CHIANTI database, except for the optically thick chromospheric lines, which are given in parentheses. The central wavelengths for Fe XV 284 Å and Fe XIV 211 Å and central wavelengths and windows for Si IV 1393 Å, Si IV 1402 Å, C II 1335 Å, H I 1216 Å (Lyα), Mg II k 2796 Å, and Mg II h 2803 Å are adopted from ?. Columns 4, 5, 6, and 7 show the basal flux, minimum and maximum values, and their physical units. 1 sfu = 10^{-22} W m⁻² Hz⁻¹. Column 8 provides the data source.

3. Results

Power-law index α as a function of T

- Line number is greatly increased
 - Allows for close inspection of temperature dependence

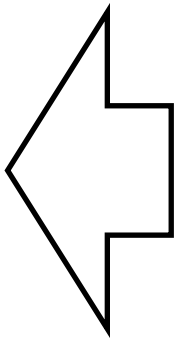
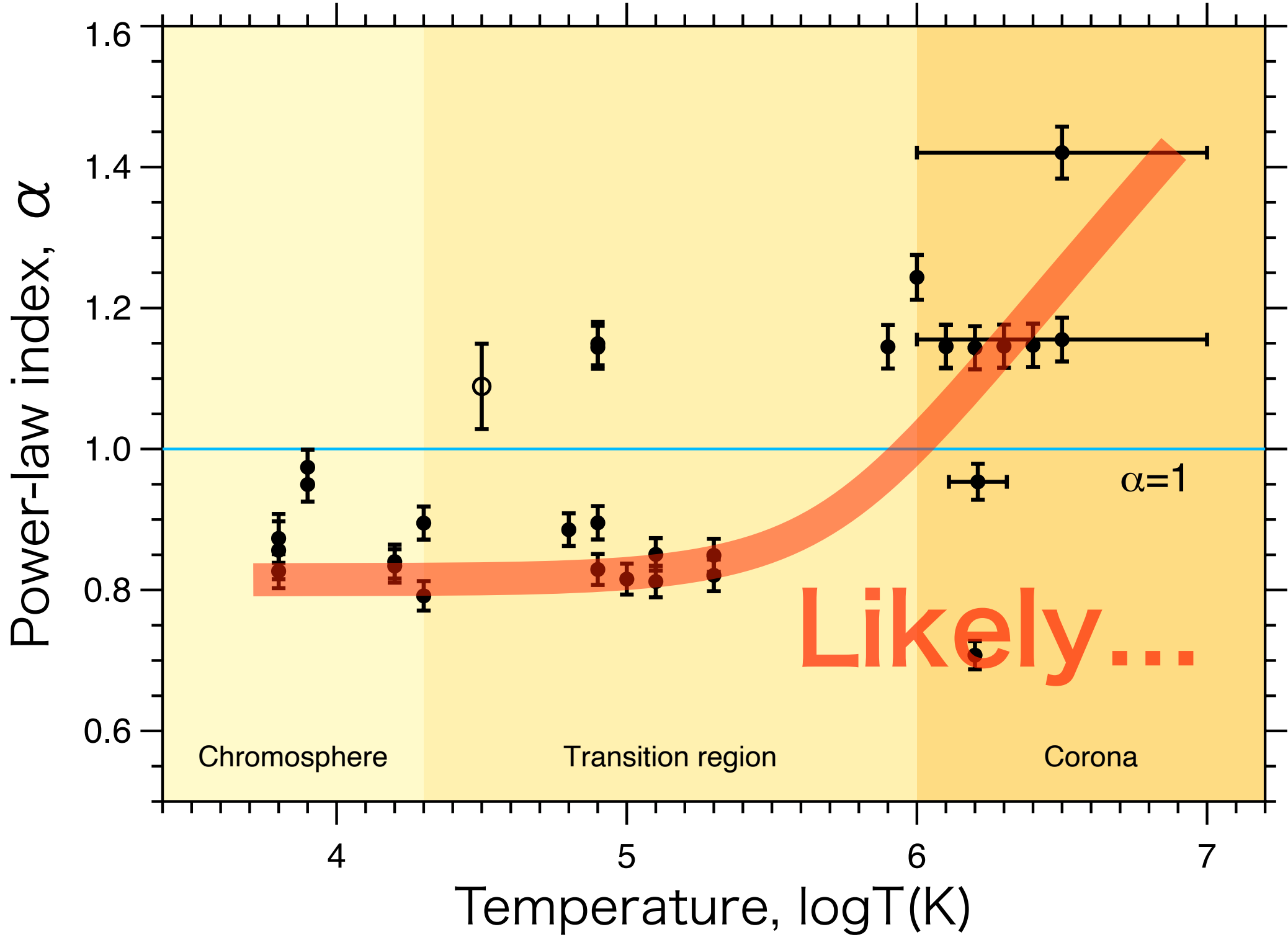


Table 1. Summary of the observables

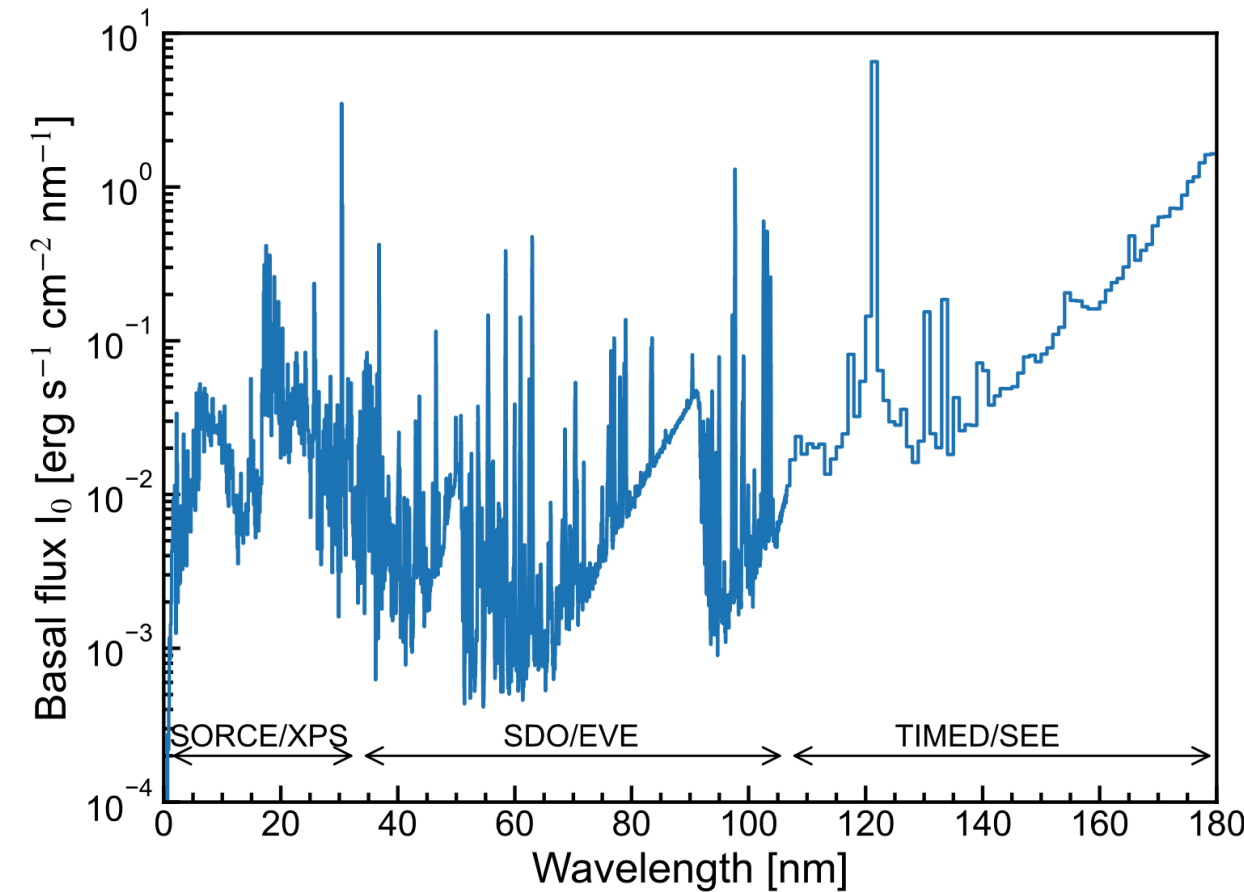
Feature	log (T/K)	Wavelength (Å)	Basal	Minimum	Maximum	Unit	Source
(1)	(2)	(3)	(4)	(5)	(6)	(7)	(8)
Radial magnetic flux	3.8	6173.3	1.18×10^{23}	1.16×10^{23}	3.35×10^{23}	Mx	SDO/HMI
LOS magnetic flux	3.8	6173.3	7.02×10^{22}	6.85×10^{22}	2.52×10^{23}	Mx	SDO/HMI
Sunspot number	3.8	WL	0	0	220	–	WDC-SILSO (ver 2.0)
Sunspot area	3.8	WL	0	0	3120	MSH	USAF/NOAA
F10.7cm radio	~6	10.7×10^8	68.83	63.67	466.57	sfu	DRAO
X-rays 1–8 Å	6–7	1–8	0	1.00×10^{-9}	4.81×10^{-5}	W m ⁻²	GOES/XRS
X-rays 5.2–124 Å	6–7	5.2–124	2.11×10^{-4}	1.85×10^{-4}	1.01×10^{-3}	W m ⁻²	SORCE/XPS
X-rays (XRT)	6.8	–	5.00×10^{-5}	4.63×10^{-5}	1.01×10^{-3}	W m ⁻²	Hinode/XRT
Fe XV 284 Å	6.4	284.15 ± 1.50	9.36×10^{-6}	5.68×10^{-6}	1.27×10^{-4}	W m ⁻²	SORCE/XPS
Fe XIV 211 Å	6.3	211.32 ± 1.50	1.20×10^{-5}	9.88×10^{-6}	6.75×10^{-5}	W m ⁻²	SORCE/XPS
Fe XII 193+195 Å	6.2	193.50 ± 2.50	6.16×10^{-5}	5.66×10^{-5}	1.72×10^{-4}	W m ⁻²	SORCE/XPS
Fe XII 1349 Å	6.2	1349.40 ± 1.00	3.64×10^{-6}	3.23×10^{-6}	5.66×10^{-6}	W m ⁻²	SORCE/SOLSTICE
Fe X 174 Å	6.1	174.53 ± 1.50	5.64×10^{-5}	5.40×10^{-5}	0.90×10^{-4}	W m ⁻²	SORCE/XPS
Fe XI 180 Å	6.1	180.41 ± 1.50	4.57×10^{-5}	4.31×10^{-5}	0.95×10^{-4}	W m ⁻²	SORCE/XPS
F10.7cm radio	~6	10.7×10^8	68.83	63.67	466.57	sfu	DRAO
Fe IX 171 Å	5.9	171.07 ± 1.50	5.50×10^{-5}	5.32×10^{-5}	0.73×10^{-4}	W m ⁻²	SORCE/XPS
N V 1238 Å	5.3	1238.90 ± 1.15	1.62×10^{-5}	1.55×10^{-5}	2.39×10^{-5}	W m ⁻²	SORCE/SOLSTICE
N V 1242 Å	5.3	1242.95 ± 1.00	1.04×10^{-5}	9.89×10^{-6}	1.54×10^{-5}	W m ⁻²	SORCE/SOLSTICE
C IV 1548 Å	5.1	1548.25 ± 1.20	1.11×10^{-4}	1.07×10^{-4}	1.53×10^{-4}	W m ⁻²	SORCE/SOLSTICE
C IV 1551 Å	5.1	1550.73 ± 0.95	6.58×10^{-5}	6.38×10^{-5}	9.02×10^{-5}	W m ⁻²	SORCE/SOLSTICE
C III 1175 Å	5.0	1175.70 ± 1.75	5.52×10^{-5}	5.35×10^{-5}	8.24×10^{-5}	W m ⁻²	SORCE/SOLSTICE
He II 256 Å+blends	4.9	256.30 ± 3.00	5.53×10^{-5}	5.20×10^{-5}	1.21×10^{-4}	W m ⁻²	SORCE/XPS
He II 304 Å	4.9	304.00 ± 1.00	4.25×10^{-4}	4.09×10^{-4}	6.19×10^{-4}	W m ⁻²	SORCE/XPS
Si IV 1393 Å	4.9	1393.85 ± 1.30	4.45×10^{-5}	4.27×10^{-5}	7.66×10^{-5}	W m ⁻²	SORCE/SOLSTICE
Si IV 1402 Å	4.9	1402.85 ± 0.85	2.32×10^{-5}	2.25×10^{-5}	3.91×10^{-5}	W m ⁻²	SORCE/SOLSTICE
Si III 1206 Å	4.8	1206.60 ± 1.25	8.59×10^{-5}	8.32×10^{-5}	1.66×10^{-4}	W m ⁻²	SORCE/SOLSTICE
He I 10830 Å	4.5	10830.40 ± 0.25	0.0292	0.0270	0.0308	W m ⁻²	SORCE/SIM & SOLIS/ISS
C II 1335 Å	4.3	1335.25 ± 1.90	1.57×10^{-4}	1.52×10^{-4}	2.46×10^{-4}	W m ⁻²	SORCE/SOLSTICE
H I 1216 Å (Lyα)	4.3	1215.70 ± 2.00	5.73×10^{-3}	5.60×10^{-3}	8.94×10^{-3}	W m ⁻²	SORCE/SOLSTICE
O I 1302 Å	4.2	1302.20 ± 0.85	4.16×10^{-5}	3.93×10^{-5}	5.40×10^{-5}	W m ⁻²	SORCE/SOLSTICE
O I 1305 Å	4.2	1305.50 ± 1.75	9.14×10^{-5}	8.77×10^{-5}	1.17×10^{-4}	W m ⁻²	SORCE/SOLSTICE
Mg II k 2796 Å	(3.9)	2796.38 ± 0.78	0.0136	0.0135	0.0180	W m ⁻²	SORCE/SOLSTICE
Mg II h 2803 Å	(3.9)	2803.48 ± 0.65	0.0097	0.0096	0.0126	W m ⁻²	SORCE/SOLSTICE
Cl I 1351 Å	(3.8)	1305.50 ± 1.75	9.06×10^{-6}	8.57×10^{-6}	1.17×10^{-5}	W m ⁻²	SORCE/SOLSTICE
Ca II K 3934 Å	(3.8)	3933.66 ± 0.50	0.0114	0.0111	0.0130	W m ⁻²	SORCE/SIM & SOLIS/ISS
Ca II H 3968 Å	(3.8)	3968.47 ± 0.50	0.0139	0.0139	0.0155	W m ⁻²	SORCE/SIM & SOLIS/ISS
H I 6563 Å (Hα)	(3.8)	6562.80 ± 0.50	0.0369	0.0360	0.0448	W m ⁻²	SORCE/SIM & SOLIS/ISS
Ca II 8542 Å	(3.8)	8542.10 ± 0.50	0.0347	0.0346	0.0392	W m ⁻²	SORCE/SIM & SOLIS/ISS

NOTE—The first column shows the features, i.e., the total unsigned radial magnetic flux and the spectral lines. The second and third columns provide the formation temperature and wavelength range, respectively, for the measurement of irradiance. The temperatures are obtained from the CHIANTI database, except for the optically thick chromospheric lines, which are given in parentheses. The central wavelengths for Fe XV 284 Å and Fe XIV 211 Å and central wavelengths and windows for Si IV 1393 Å, Si IV 1402 Å, C II 1335 Å, H I 1216 Å (Lyα), Mg II k 2796 Å, and Mg II h 2803 Å are adopted from ?. Columns 4, 5, 6, and 7 show the basal flux, minimum and maximum values, and their physical units. 1 sfu = 10^{-22} W m⁻² Hz⁻¹. Column 8 provides the data source.

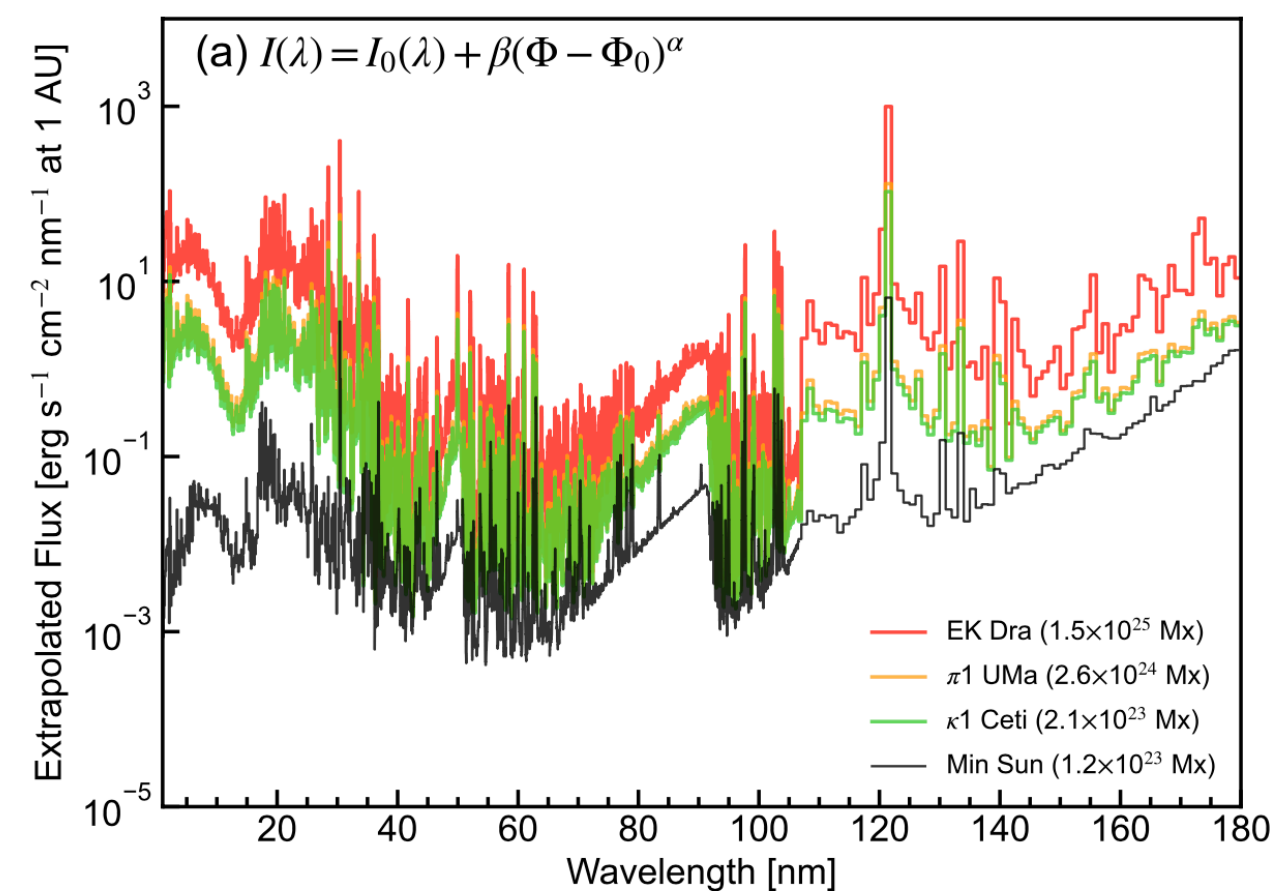
4. Discussion and Perspectives

- Impacts on exoplanets: XUV modeling

Observation: solar spectra



Simulation: modeled spectra for G dwarfs



- This study: Mag flux vs irradiance for **each line**

$$I^{\text{line}} = \beta (\Phi - \Phi_0)^\alpha + I_0^{\text{line}}$$



- Namekata et al: Mag flux vs irradiance for the **whole XUV spectrum** with a wavelength resolution of 1 Å bin
- XUV spectra: 1 Å ~ 1800 Å

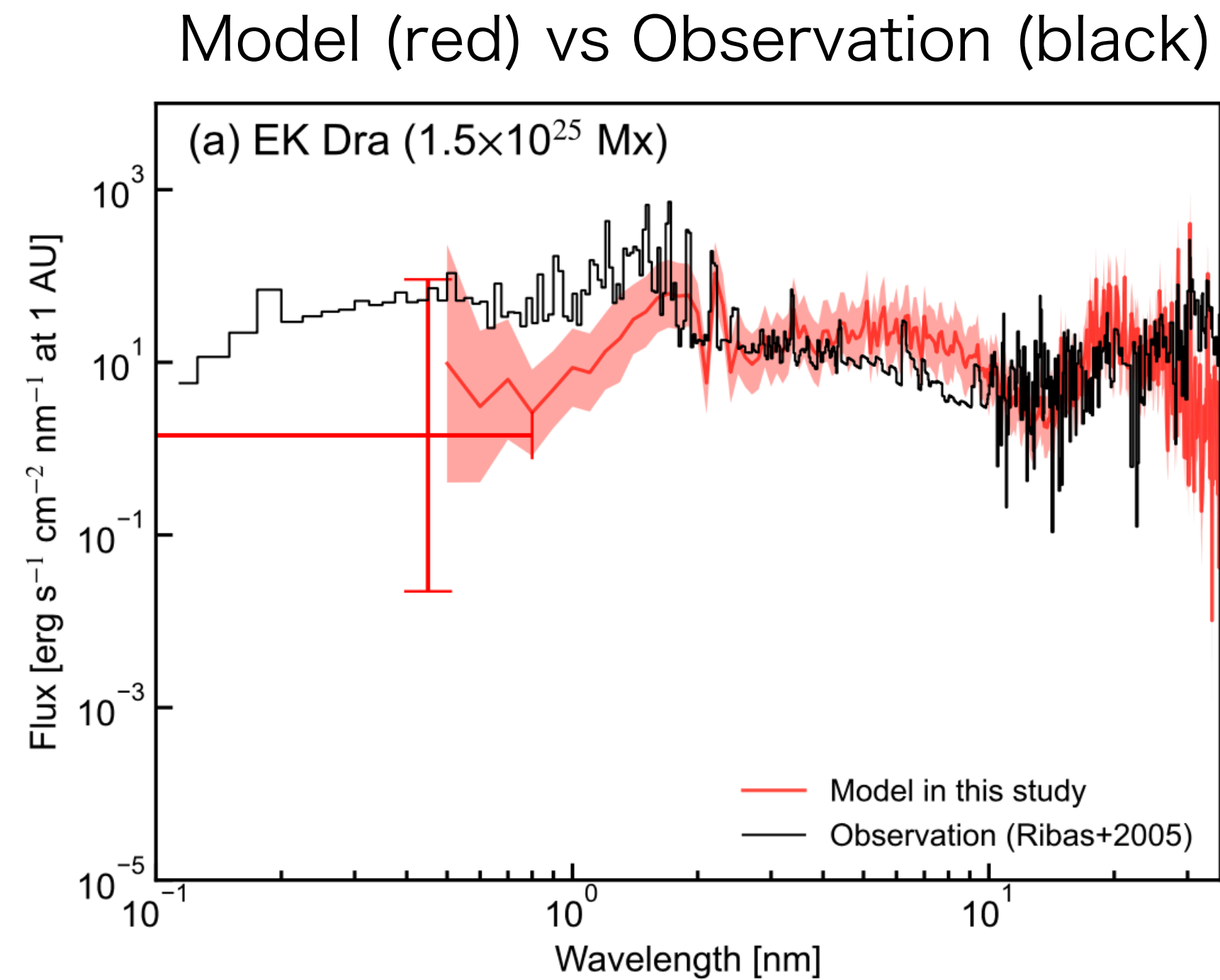
$$I(\lambda) = \beta (\Phi - \Phi_0)^\alpha + I_0(\lambda)$$



- Provide **synthesized XUV spectra** for G-dwarfs based on observed magnetic fluxes
- Maybe utilized as inputs for chemical calculations of exoplanetary atmospheres

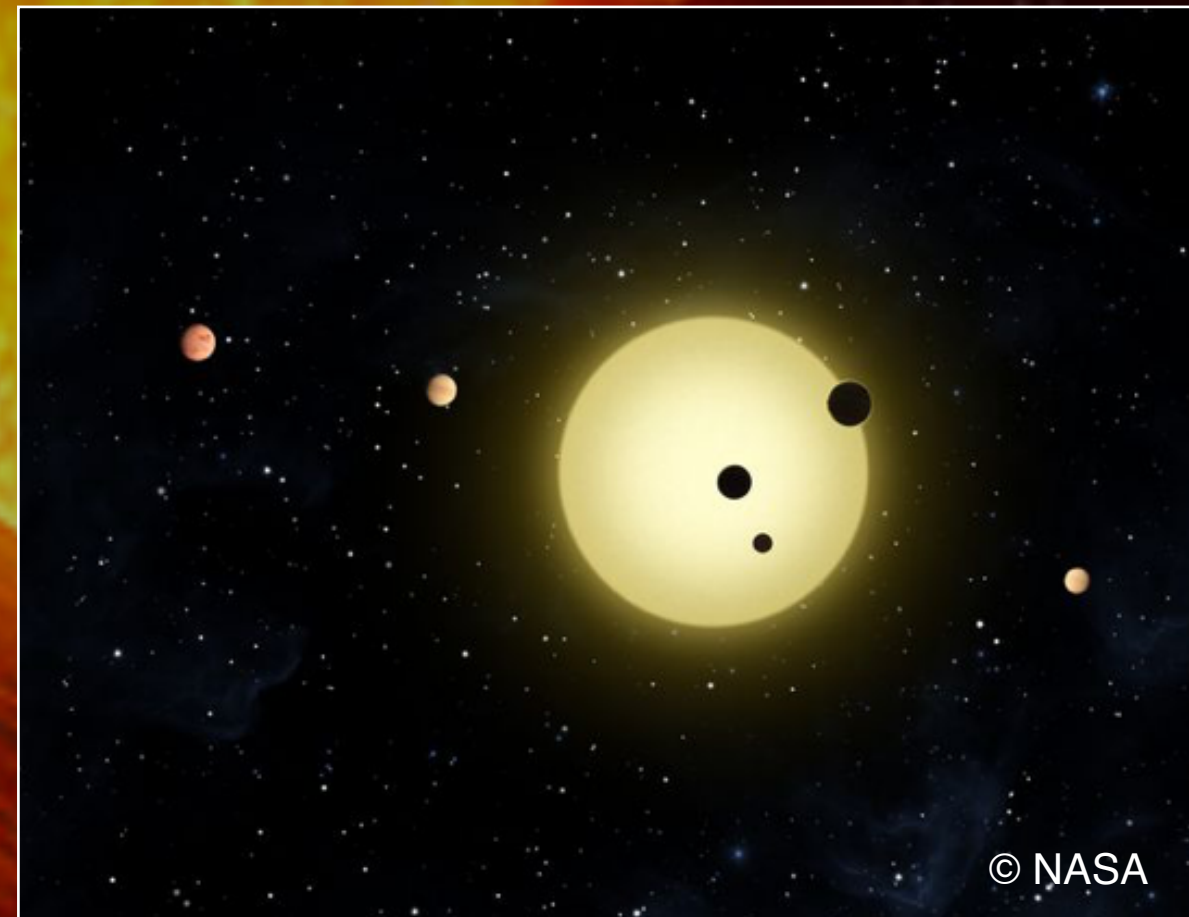
4. Discussion and Perspectives

- Impacts on exoplanets: XUV modeling



- Overall consistent with observed spectra
- For active young stars, deviations are seen particularly on the shorter wavelength range

- Limited observations of stars in XUV
- Important to perform **simultaneous multi-wavelength observation over a long period of time and in multiple phases**



5. Summary

• Analysis

- Comparison of **scaling laws** $F \propto \Phi^\alpha$ **between the Sun and Sun-like stars** with ages from 50 Myr to 4.5 Gyr

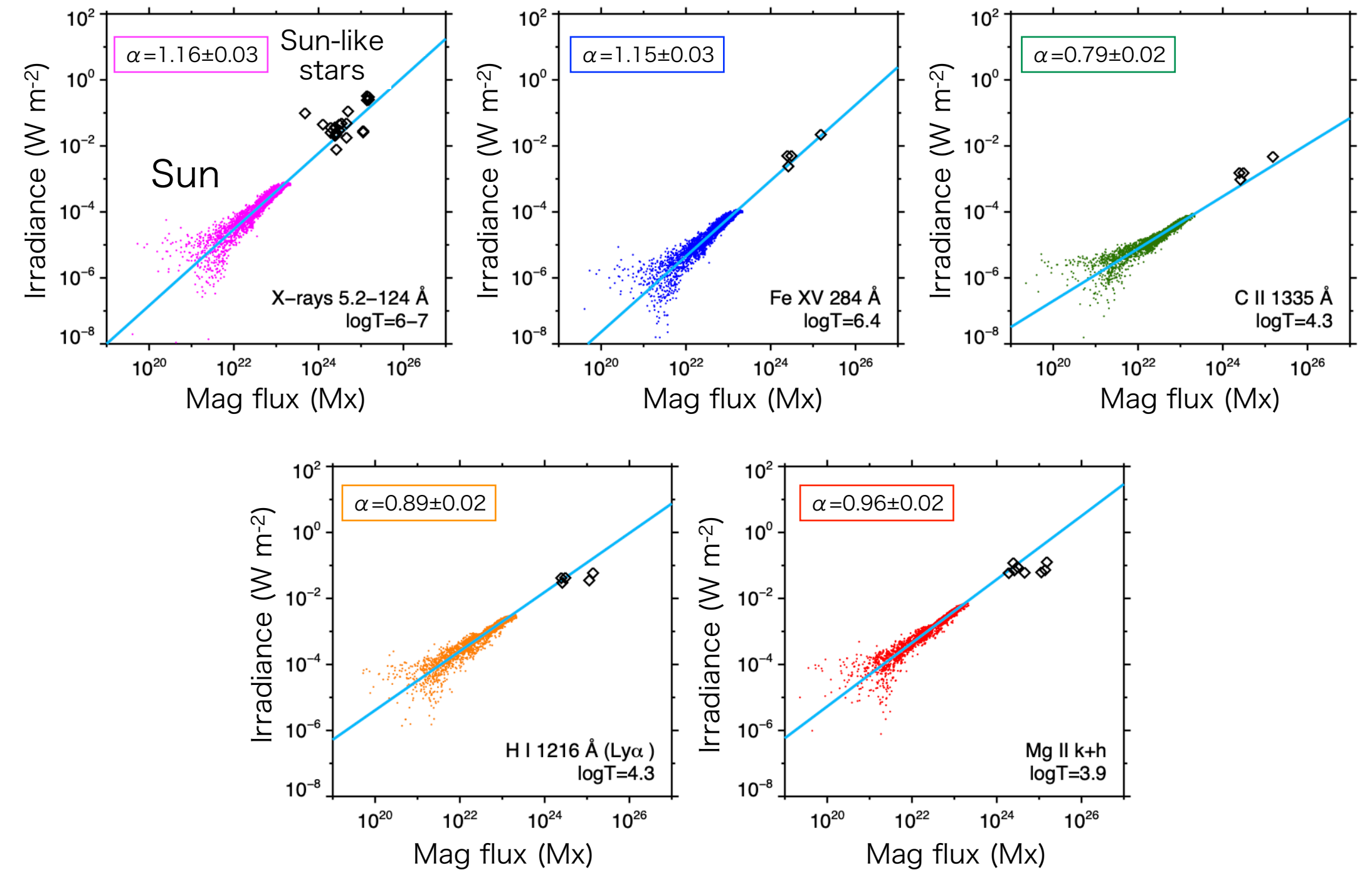
• Results

- The scaling relations are **consistent in any wavelength domains (= temperatures)**
- α decreases from above- (corona) to below-unity (chrom)

• Conclusion

- **The heating mechanism is universal among the Sun and Sun-like stars, regardless of age or activity**
- Variation in α for different temperatures may indicate difference in heating mechanisms
- Now working on **empirical XUV spectra modeling**

Mag flux—multi-line proportionality $F \propto \Phi^\alpha$



Toriumi & Airapetian 2022, ApJ, 927, 179

<https://doi.org/10.3847/1538-4357/ac5179>

Thank you for your attention

Send feedback to toriumi.shin@jaxa.jp